Published at Materials Science and Technology, http://dx.doi.org/10.1080/02670836.2017.1327563

Fabrication of Nanostructured Pearlite Steel Wires Using Electropulsing

Rongshan Qin [1,2], Yongkun Luo[2], Bernadette Elliott-Bowman[2], Osamudiamen Omoigiade [2]

1. School of Engineering and Innovation, The Open University, Walton Hall, Milton Keynes MK7 6AA, UK

2. Department of Materials, Imperial College London, Exhibition Road, London SW7 2AZ, UK

Abstract: This work reports the refinement of pearlite structure into nanostructure using electropulsing. Nanostructured pearlitic steel wires possess nanoscale lamellae or nanoscale grain microstructures. Fabrication of nanostructures by severe plastic deformation and lamellar to grain transformation have been investigated. It is suggested that an aligned pearlite structure is preferred in severe plastic deformation. The lamellar to grain transformation is controlled by diffusion of carbon within cementite and also from cementite to ferrite phases. Carbon mobility is changed by mechanical, thermal and electrical states. The interface between nanoscale sub-grains in the ferrite phase has considerable carbon content. Numerical calculations and experimental observations demonstrated these mechanisms.

Keywords: Steel wires, Pearlite, Nanostructure

Introduction

Pearlite steel wires are applied broadly in engineering for their high tensile strength, high fatigue resistance, high wear durability and other merit mechanical properties. Fabrication of nanostructured pearlite steel wires has attracted significant attention due to the potential good performance of nanostructured materials [1-6]. Nanocrystalline metals and alloys increase strength and resistance to tribological damage and crack propagation [2-4]. A tensile strength of 7 GPa has been achieved in a nanostructured steel wire by severe drawing of a pearlite steel in a laboratory [1]. The redistribution of carbon from the cementite phase to the interface between ferrite sub-grains has been observed by atom probe tomographic characterization, which plays an important role in the fabrication of nanostructures and nano-domains [1, 7]. The nanostructured lamellar pearlite can be obtained by controlling chemical and thermal processing conditions, where the migration of the ferrite-cementite interface has been controlled by addition of aluminium and cobalt to steels [5]. The nanostructured cementite

*Corresponding author, email rongshan.qin@open.ac.uk

grains have been fabricated by electropulsing treatment of a cold-drawn pearlite steel wire at ambient temperature [6]. The formation of nanoscale cementite particles are related to carbon diffusion driven by an electric field and thermal state. Control of the carbon diffusion in a carbon-supersaturated ferrite phase has also been applied in fabrication of other nanostructured steels [8].

This work investigates the problems and possible solutions in fabrication of nanoscale lamellae by severe drawing of pearlite wire. It will be shown that severe plastic deformation (SPD) does not always help to reduce pearlite interlamellar spacing. Such a problem can be overcome by designing an aligned pearlite microstructure. In the fabrication of nanoscale grain structures using lamellar to grain transformation (LGT), the mechanisms for carbon diffusion within cementite to form nanoscale cementite grains and diffusion from cementite to ferrite sub-grain interfaces have been investigated. The influences of mechanical, thermal and electrical state on the development of nanostructures have been studied.

Lamellar Nanostructure

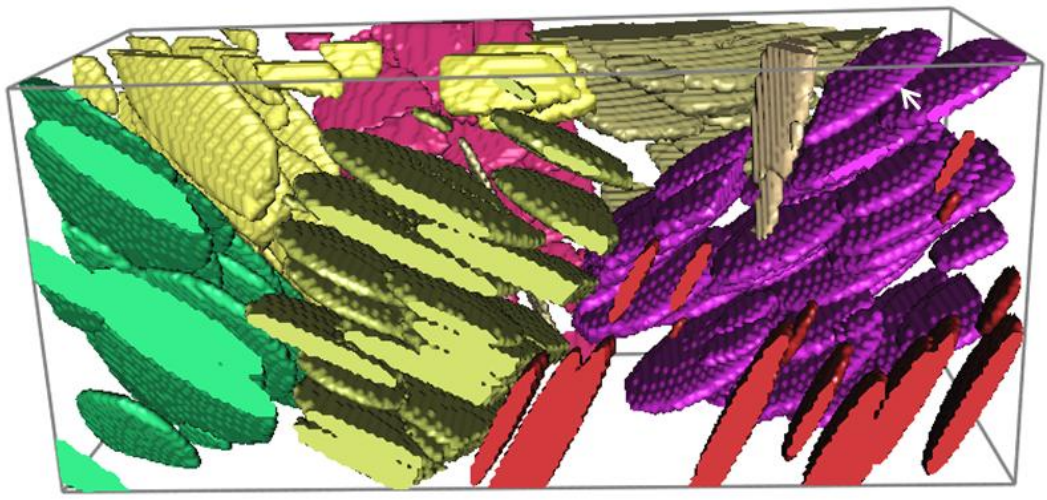

Figure 1. A pearlite steel microstructure obtained by phase-field calculation and plotted by an in-house visualization code package MatVisual. The plates are the cementite phase, and the spaces between them are the ferrite phase.

Pearlite steel contains body-centred-cubic ferrite iron and orthorhombic iron carbide cementite (Fe_3C). In the austenite-pearlite phase transformation, ferrite and cementite bi-

crystals grow from the parent austenite grain. The orientation between cementite and ferrite obeys Pitsch-Petch relationship of $(001)_{Fe_3C}$ //$(5\bar{2}\bar{1})_{bcc}$, $(010)_{Fe_3C}$ $2°-3°$ from $(11\bar{3})_{bcc}$ and $(100)_{Fe_3C}$ $2°-3°$ from $(13\bar{1})_{bcc}$ [9]. Figure 1 shows a distribution of cementite plates from our computer simulation. The space between cementite plates are ferrite phase. The microstructure was generated following a phase-field calculation [10-11] and plotted using a visualization code package MatVisual. An arrow representing a vector is placed near to the right-top in figure 1. The magnitude of the vector represents the pearlite lamellar spacing (*d*). In homogeneous wire drawing, a vector is changed from $\vec{u}$ to $\vec{v}$ by following transformation [12], where *s* is the equivalent strain.

$$\begin{pmatrix} s & 0 & 0 \\ 0 & 1/\sqrt{s} & 0 \\ 0 & 0 & 1/\sqrt{s} \end{pmatrix} \begin{pmatrix} u_1 \\ u_2 \\ u_3 \end{pmatrix} = \begin{pmatrix} v_1 \\ v_2 \\ v_3 \end{pmatrix} \quad (1)$$

When the vector in Figure 1 is perpendicular to the wire drawing direction, the original pearlite lamellar spacing (*d*) will be reduced to $d/\sqrt{s}$. Severe drawing ($s>1$) can reduce the pearlite interlamellar spacing and help to fabricate a lamellar pearlite nanostructure. However, when the vector is parallel to the drawing direction, the pearlite lamellar space (*d*) will be increased to $d \cdot s$. In such cases the severe plastic deformation might change the nanostructured lamellar pearlite into a coarsened microstructure. Therefore, the ideal case is to have all the cementite and ferrite plates in pearlite aligned in the wire drawing direction.

Table 1. Anisotropic surface energy of Fe_3C crystal

Orientation	(1 0 0)	(0 1 1)	(0 1 0)	(1 0 1)	(1 1 1)	(1 1 0)	(0 0 1)
Surface energy (J/m^2)							
Ref [15]	2.47	2.37	2.26	2.25	2.22	2.19	2.05
Eq. (2)	2.4677	2.2515	2.2742	2.2609	2.2497	2.2554	2.0506
Relative error (%)	0.09	5.00	0.63	0.49	1.34	2.99	0.03

Given the Pitsch-Petch relationship in pearlite growth, the crystallographic orientations of cementite plates are fixed after the nucleation of cementite crystals. It is known that interface anisotropy has significant contribution towards crystal morphology [10, 13]. In many cases, the crystallographic orientation determines the crystal morphology [10, 14]. The anisotropic surface energy of cementite has been calculated using a gradient-corrected pseudopotential-

based density functional theory [15]. Their results are listed in Table 1. Cementite has an orthorhombic crystal structure and Pnma (No.62) space group. Its lattice parameters are *a* = *5.06* Å, *b* = *6.74* Å and *c* = *4.51* Å and angles α=β=γ= 90° respectively [16]. From symmetry analysis, we can represent the anisotropic surface energy of cementite orthorhombic crystal using

$$\sigma(\hat{n}) = 2.21537 + 0.238931 n_x^4 + 0.0692452 n_y^4 - 0.15528 n_z^4 \tag{2}$$

where

$$n_x = ah / \sqrt{(ah)^2 + (bk)^2 + (cl)^2} \tag{3}$$

$$n_y = bk / \sqrt{(ah)^2 + (bk)^2 + (cl)^2} \tag{4}$$

$$n_z = cl / \sqrt{(ah)^2 + (bk)^2 + (cl)^2} \tag{5}$$

h, *k* and *l* are Miller indices. The values in several orientations are listed in Table 1. The largest relative error is 5% in (011) direction. The polar diagram of anisotropic surface energy of cementite is plotted in Figure 2(a). It can be seen that the anisotropy is sufficiently weak. Figures 2(b)-(c) illustrate the morphology of cementite crystal grown freely, that is, in unrestrictive conditions. The anisotropy-induced crystal morphology is not far from isotropic. This shows that the crystallographic relationship has negligible effect on the morphological orientation of cementite crystals. Other effects can be implemented to generate the desirable cementite microstructure.

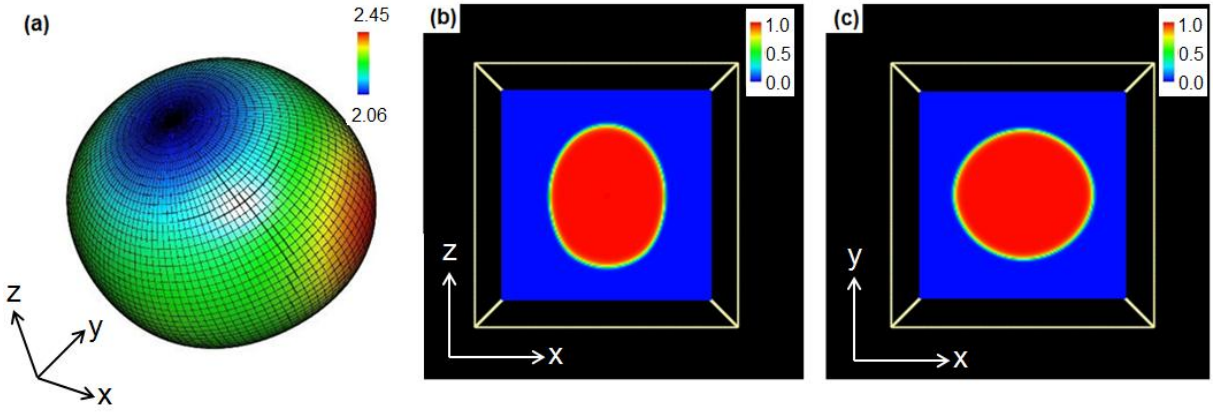

Figure 2. (a) Polar diagram of cementite surface energy; (b) and (c) the morphology of a cementite crystal grown in unrestricted space at x-z plane and x-y plane, respectively

The morphological orientation of pearlite can be controlled by the migration direction of the ferrite-cementite interface. Electric current aids the development of this interface along the electric current direction. Klinger and Levin have analysed the interface stability under

electric field and proved theoretically that the electric current promotes the development of an interface along the direction of the electric field [17]. The same suggestion has been made by thermodynamic consideration of effect of electric current on microstructure evolution [18]. We have observed this tendency experimentally in low carbon steels [19], and are working toward the fabrication of aligned fully pearlite high carbon steel wire.

Lamellar to grain nanostructure transformation

Deformation and recrystallization can induce a lamellar to grain nanostructure transformation, where carbon atoms in cementite are transported to ferrite phase by mechanical alloying and subsequently precipitate to the interface between nanoscale ferrite sub-grains [1]. Our previous work shows that passing electric current at ambient temperature to a cold-drawn pearlite steel wire causes the formation of nanostructured cementite, where the mechanism was attributed to the deformation and electropulse-promoted low-temperature recrystallization [6]. In the present study, an experiment has been designed to identify whether the cold-drawn state is a necessary condition for such nanostructure transformations to progress. The electric current pulses have been applied to an annealed pearlite steel wire. The cold-drawn effects, such as the excess dislocation density and residual stress, have been removed by the annealing. The samples were prepared and annealed at TATA Steel Swinden Technology Centre, then sent to us for electropulsing treatment. The wire with one end was submerged in warm water and another in liquid nitrogen. The wire was electropulsed with 200A peak amplitude current, 200μs pulse width at 10Hz for 600s. Figure 3 (a)-(b) are the Scanning Electron Microscopy (SEM) images of the electropulsing treated samples after 2% Nital etching. The as-received microstructure was a conventional pearlite lamellar microstructure with lamellar spacing $d = 40$ nm. The electric current pulses have caused the lamellar cementite to transform into nanoscale grains. The electropulsed microstructure in the annealed samples is similar to that of the cold-drawn samples. The latter result, plotted in Figure 3(c)-(d) was obtained by cold-drawn pearlite steel wires provided by POSCO at South Korea [6]. It is proved that the cold-working is unnecessary for the promotion of cementite fragmentation and spheroidization. However, electropulsing the cold-drawn pearlite steel wire generate more thorough grain nanostructure than that of the annealed wire. For examples, the areas labelled A and B are not completely fragmented. It retains the as-received lamellar pearlite microstructure. These lamellae are almost parallel to the electric current direction, as labelled as an arrow in Figure 3(a). This means that the lamellae perpendicular to the electric current

direction are easier to transform into grain structure than that of parallel ones. This is in agreement with our previous experimental observations in other steels [18-19].

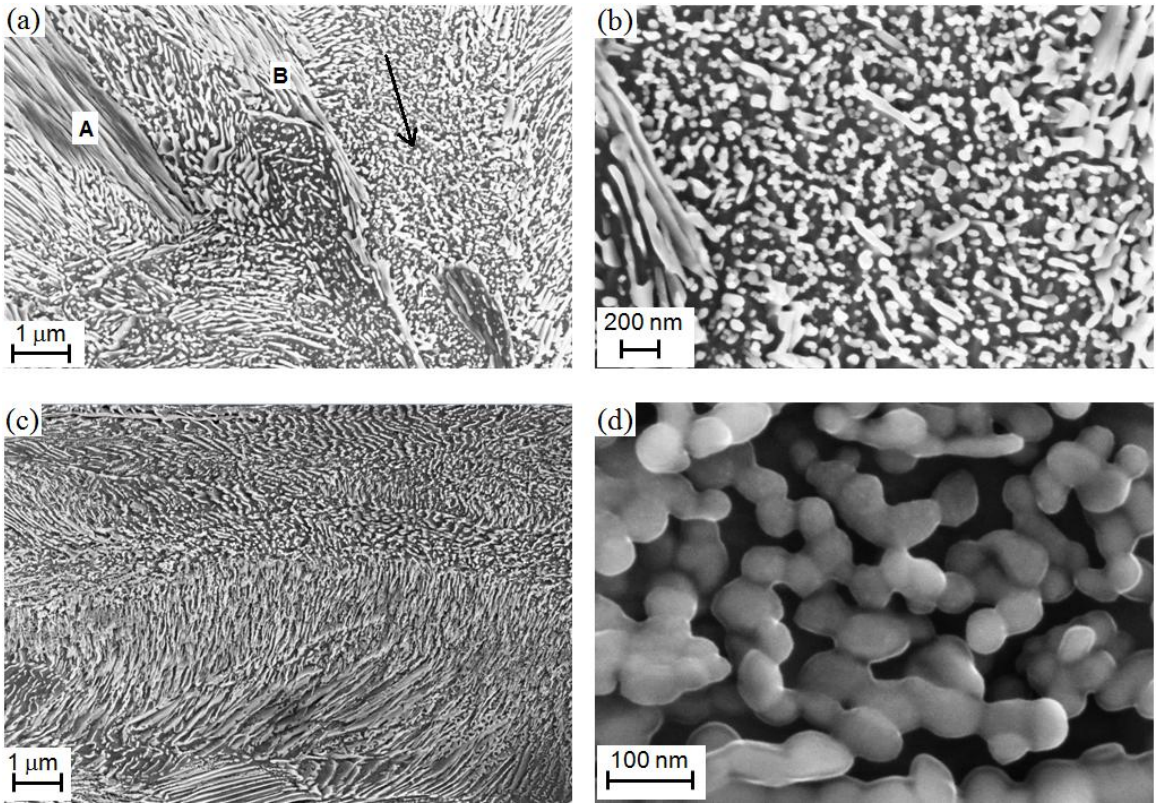

Figure 3. SEM images of (a)-(b) annealed steel after electropulsing treatment; (c)-(d) the cold-drawn steel after electropulsing treatment

To study the influence of the physical environment around cementite plates during electropulsing treatment, numerical calculation has been performed on a disk cementite plate submerged in ferrite matrix. The theory and discretization method has been described in other papers [20]. The parameters for electrical resistivity of ferrite and cementite are 9.17×10^{6} S·m^{-1} and 1.22×10^{6} S·m^{-1}, and for magnetic permeability of ferrite and cementite $300\mu_0$ and $30\mu_0$, respectively, where $\mu_0 = 1.26\times10^{-6}\, N\cdot A^{-2}$ is the vacuum permeability [21-24]. Figure 4(a) and 4(b) show the temperature distribution around a thin cementite disk which is parallel and perpendicular to the electric current direction, respectively. Figure 4(c) and 4(d) show electric current density distributions around a cementite disk. It can be seen clearly that electric current increases the temperature of cementite more than that of the ferrite, as illustrated in figure 4(a) and 4(b). It is reasonable to suggest that a sudden higher temperature rise in cementite than that of ferrite causes more volume expansion of cementite and hence a higher local stress in cementite. Carbon atoms are pushed away from the area of high local stress, similar to the graphite squeezed out of austempered ductile cast iron [25]. The high local

temperature in cementite also provides a high carbon mobility to facilitate diffusion and spheroidization. Furthermore, it is seen that the cementite in Figure 4(a) experiences a much higher temperature rise than Figure 4(b). The cementite plate in Figure 4(a) is perpendicular to the current direction and in Figure 4(b) is parallel to the current direction. This provides an explanation for the un-fragmented cementite lamellae when they are parallel to the current direction. The lamellae perpendicular to the current direction cause more severe mechanical and thermal elavations than that of the parallel ones when electric current passes the pearlite steel wire. Figure 4(c) and 4(d) demonstrate the electric current density distributions. It can be seen that Figure 4(c) has higher electric current passing through the cementite disk than that of Figure 4(d). The effect of electromigration on the carbon diffusion is stronger when cementite plate is perpendicular to the current flow than that of the parallel ones. The high mechanical, thermal and electric effects promote carbon diffusion, which leads to the spheroidization of cementite and also of carbon into ferrite phase. The breakup of cementite plates has also been promoted by the electric current. A thermodynamic calculation of the current-induced breakup has been published in another journal recently [26].

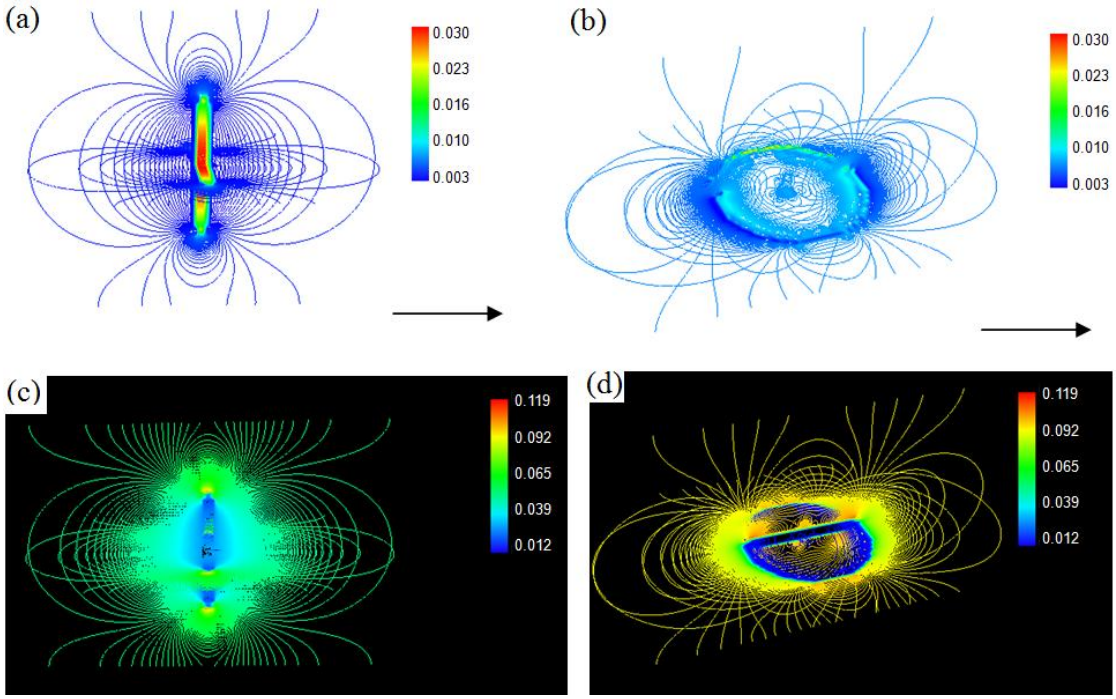

Figure 4. Joule heating-caused temperature rising when a cementite disk is (a) perpendicular to, and (b) parallel to the electric current direction; The electric current density distribution in pearlite when a cementite disk is (c) perpendicular to, and (d) parallel to the electric current direction. The arrows represent the electric current direction.

However, the microstructural information on ferrite has not been revealed in Figure 3. The reason is that 2% Nital etching liquid etched away ferrite phase in the nanostructured pearlite. In order to investigate this, we acquired some pearlitic rail steel samples from TATA Steel Teesside Technology Centre. The samples were cut from an ingot and then cold rolled to thin plates before treatment with electropulses. The pearlite interlamellar spacing is around 400 nm. The electropulsed samples were etched by Marshall's reagent for SEM characterization. The results are demonstrated in Figure 5(a)-(b). The ferrite lamellae have been fragmented into finer ferrite grains. Figure 5(c) shows the carbon distribution across the ferrite lamellae by atom probe tomographic characterization. It can be seen that the interface between ferrite grains contains high carbon composition. So far, we are not sure whether the lamellar to grain transformation in ferrite is caused by cold rolling or electropulsing treatment of the samples, because some grain ferrite were also noticed in the cold-rolled samples before electropulsing. However, the diffusion of carbon from cementite to the interface has been surely promoted by the electropulsing treatment.

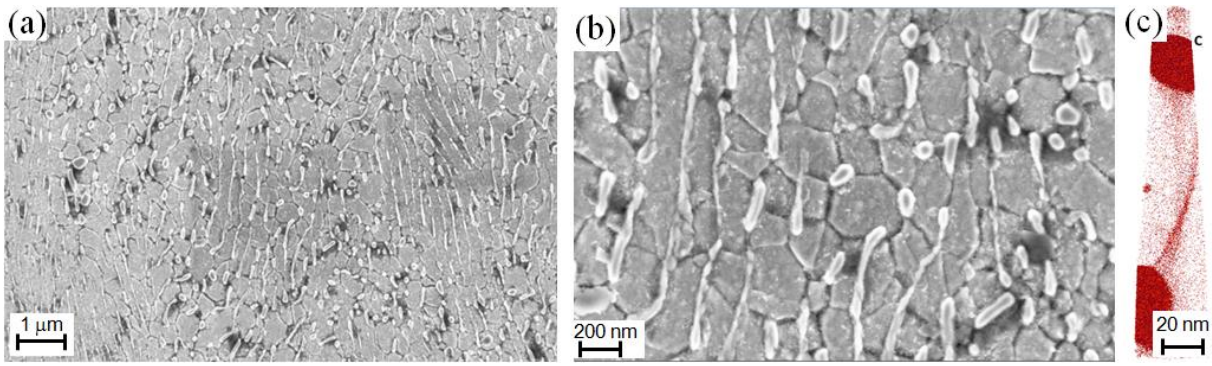

Figure 5. (a)-(b) SEM images for the electropulsed pearlite steel. (c) Atom probe tomographic image shows the carbon distribution between ferrite grains.

Similar microstructures to figure 5(b) have been reported in literature by other treatment methods. One of the cases is by equal channel angular pressing of a fully pearlitic Fe–0.8C steel at 923K [27]. Another example is after laser shock processing of high carbon pearlitic steel [28].

Conclusions

In the present work, the fabrication of nanostructured pearlite wire using electropulsing has been discussed. In nanoscale lamellar pearlite processing, severe plastic drawing is not always helpful for reducing the pearlite lamellar spacing. An aligned pearlite microstructure with

cementite and ferrite plates along the wire's axial direction is preferred. Due to the low anisotropy of cementite surface energy, fabrication of aligned pearlite is possible by control the external field gradient. In fabrication of nanostructured grain pearlite steel wire, carbon diffusion within cementite during spheroidization and from cementite to the interface of ferrite grains plays an important role in nanoscale lamellar to grain transformation. The diffusion is affected by mechanical, thermal and electrical heterogeneities.

Acknowledgements

We are grateful for A. Haldar, S. Hobson and P. Bradley from TATA Steel for providing of steel wire samples. The work was sponsored by POSCO, TATA Steel (1322018) and DSTL (DSTLX1000064117).

References

1. Li YJ, Raabe D, Herbig M, et al. Segregation stabilizes nanocrystalline bulk steel with near theoretical strength. Phys Rev Lett. 2014; 113: 106104.
2. Kumar KS, Van Swygenhoven H, Suresh, S. Mechanical behavior of nanocrystalline metals and alloys. Acta Mater. 2003; 51: 5743-5774.
3. Meyers MA, Mishra A, Benson, DJ. Mechanical properties of nanocrystalline materials. Prog Mater Sci. 2006; 51: 427-556.
4. Hanlon T, Tabachnikova ED, Suresh S. Fatigue behavior of nanocrystalline metals and alloys. Inter J Fatigue. 2005; 27: 1147-1158.
5. Wu KM, Bhadeshia, HKDH. Extremely fine pearlite by continuous cooling transformation. Scr Mater. 2012; 67: 53-56.
6. Qin RS, Samuel EI, Bhowmik A. Electropulse-induced cementite nanoparticle formation in deformed pearlitic steels, J Mater Sci. 2011; 46: 2838-2842.
7. Li YJ, Choi P, Goto S, et al. Evolution of strength and microstructure during annealing of heavily cold-drawn 6.3 GPa hypereutectoid pearlitic steel wire. Acta Mater. 2012; 60: 4005-4016.
8. Bhadeshia HKDH. Nanostructured bainite. Proc R Soc A. 2010; 466: 3-18.
9. Zhou DS, Shiflet GJ. Ferrite: Cementite crystallography in pearlite. Metall Trans A. 1992; 23: 1259-1269.
10. Qin RS, Bhadeshia HKDH. Phase-field model study of the effect of interface anisotropy on the crystal morphological evolution of cubic metals. Acta Mater. 2009; 57**:** 2210-2216.

11. Granasy L, Pusztai T, Borzsonyi T, et al. A general mechanism of polycrystalline growth. Nat. Mater. 2004; 3: 645-650.
12. Zhu Q, Sellars CM, Bhadeshia HKDH. Quantitative metallography of deformed grains. Mater Sci Technol. 2007; 23: 757-766.
13. Luo YK, Qin, RS. Influences of the third and fourth nearest neighbouring interactions on the surface anisotropy of face-centred-cubic metals. SURF SCI. 2014; 624: 103-111.
14. Qin RS, Bhadeshia HKDH. Phase-field model study of the crystal morphological evolution of hcp metals. Acta Mater. 2009; 57**:** 3382-3390.
15. Chiou WC, Carter EA. Structure and stability of Fe3C-cementite surfaces from first principles, Surf Sci. 2003; 530: 87–100.
16. Herbstein FH, Smuts J. Comparison of X-ray + neutron-diffraction refinements of structure of cementite Fe_3C. Acta Cryst. 1964; 17: 1331-1332.
17. Klinger L, Levin L. Interface instability in an electric field. J App Phys. 1995; 78: 1669–1672.
18. Zhao ZC, Qin RS. Inclusion agglomeration in electrified molten metal: thermodynamic consideration. Mater Sci Technol. 2017; DOI: 10.1080/02670836.2016.1270729
19. Rahnama A, Qin RS. Electropulse-induced microstructural evolution in a ferritic-pearlitic 0.14% C steel. Scr Mater. 2015; 96: 17-20.
20. Qin RS, Bhowmik A. Computational thermodynamics in electric current metallurgy. Mater Sci Technol. 2015; 31: 1560-1563.
21. Bohnenkamp U, Sandström R, Grimvall G. Electrical resistivity of steels and face-centered-cubic iron. J Appl Phys. 2002; 92: 4402-4407.
22. Zhang P, Wang XB, Wang W, et al. Iron carbide and nitride via a flexible route: synthesis, structure and magnetic properties. RSC Adv. 2015; 5:21670-21674.
23. Thompson SM, Tanner BK. The magnetic-properties of pearlitic steels as a function of carbon content. J Magn Magn Mater. 1993; 123: 283-298.
24. Hao XJ, Yin W, Strangwood M, Peyton AJ, et al. Off-line measurement of decarburization of steels using a multifrequency electromagnetic sensor. Scr Mater. 2008; 58: 1033-1036.
25. Myszka D, Wasiluk K, Skolek E, et al. Nanoausferritic matrix of ductile iron. Mater Sci Technol.2015; 31: 829-834.
26. Qin R. Using electric current to surpass the microstructure breakup limit. Sci Rep. 2017; 7: 41451.

27. He TT, Xiong Y, Ren FZ, et al. Microstructure of ultra-fine-grained high carbon steel prepared by equal channel angular pressing. Mater Sci Eng A. 2012; 535: 306–310.
28. Xiong Y, He TT, You L, et al. Microstructure and microhardness of pearlitic steel after laser shock processing and annealing. Mater Sci Technol. 2016; 31:1825-1831.